Advances in Engineering Software, Vol.20, No.1, pp. 19-27, 1994

Boundary Element Methods for 3D Capacitance and Substrate Resistance Calculations in Inhomogeneous Media in a VLSI Layout Verification Package

T. Smedes, N.P. van der Meijs and A.J. van Genderen

Delft University of Technology, Faculty of Electrical Engineering, P.O. Box 5031, NL-2600 GA Delft the Netherlands

ABSTRACT

In this paper we describe the application of the Boundary Element Method to the layout verification of VLSI Designs. We describe the methods for the calculation of interconnection capacitances and substrate resistances with the use of problem specific Green's functions. The derivation of these functions for multilayer structures is presented. Emphasis is on computational efficiency and practical accuracy. These are achieved by the type of the Green's functions and an appropriate model reduction technique. The methods are implemented in the layout extractor Space.

Keywords: Boundary Element Method, Green's function, Integrated Circuit, layout verification, capacitance calculation, substrate resistance calculation.

INTRODUCTION

Designers of modern VLSI circuits heavily rely on layout-to-circuit extractors, which translate a chip layout into an equivalent network suitable for electrical verification of their layouts. Because of the growing influence of parasitic elements, such extractors must be able to model (extract) more and more parasitic phenomena. Parasitic capacitances and coupling between different components via the substrate of the chip are severe problems.[1,2] We describe Boundary Element Methods for the calculation of interconnection capacitances and substrate resistances for the layout-to-circuit extractor Space.[3] These components are indicated in Figure 1. We do not attempt to solve a *field* problem for a given set of boundary conditions. Instead we want to obtain a *circuit model* for the given physical situation. In particular we seek the capacitance matrix $\mathbf{C}_s$ for the interconnect and the indefinite admittance matrix $\mathbf{Y}_{\mathrm{IAM}}$ for the substrate.

BOUNDARY ELEMENT FORMULATION

The problems mentioned above are generally described by the equation

$$\nabla(K\nabla u) = 0 \qquad \text{on a domain } \Omega, \tag{1}$$

where u denotes the potential and K is a parameter of the medium. All problems addressed in this paper are described by a domain with parallel layers of constant K. This is illustrated in Figure 1. For constant K this equation reduces to the Laplace equation.

For the capacitance problem the domain is the semi-infinite layered halfspace above the silicon. K is the permittivity (ϵ) of the domain. The domain contains M conductors with inhomogeneous Dirichlet conditions. Homogeneous Dirichlet conditions hold at the groundplane and infinity. The unknowns are the charges on the conductors.

For the resistance problem the domain is a layered cuboid with conductivity $K = 1/\rho$. The substrate is contacted by P contacts with inhomogeneous Dirichlet conditions. The contacts can be positioned on the silicon-dielectric interface and at the bottom of the substrate. Homogeneous Neumann conditions hold on the remainder of the boundary. The unknowns are the currents through the contacts.

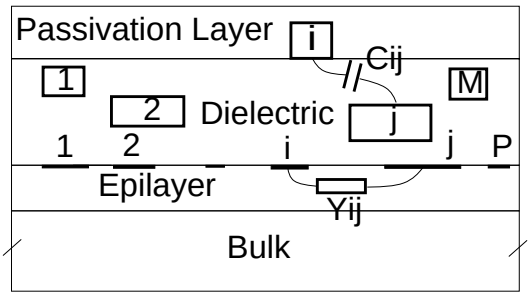

- dielectric, containing M conductors:
  passivation, silicon nitride, $\epsilon_r = 7.5$.
  dielectric, silicon oxide, $\epsilon_r = 3.9$.
- silicon with P contacts on the boundary:
  epi-layer, low-doped, $\rho = 15\ \Omega$cm.
  bulk, high-doped, $\rho = 0.05\ \Omega$cm.

Figure 1: *Cross section of a chip with a possible succession of layers.*

The above problems may be rewritten as a boundary integral equation[4]

$$\alpha u + \int_{\Gamma_1} \overline{u}\frac{\partial u^*}{\partial n} d\Gamma + \int_{\Gamma_2} u\frac{\partial u^*}{\partial n} d\Gamma = \int_{\Gamma_1} \frac{\partial u}{\partial n} u^* d\Gamma + \int_{\Gamma_2} \overline{\left(\frac{\partial u}{\partial n}\right)} u^* d\Gamma \quad (2)$$

where overlined quantities are prescribed by boundary conditions and u^* is a fundamental solution or the (free space) Green's function. Γ_1 denotes the part of the boundary with Dirichlet conditions and Γ_2 denotes the part of the boundary with Neumann conditions. Green's function satisfies

$$\nabla^2 u^*(\vec{x}; \vec{x_s}) = -\frac{\delta(\vec{x} - \vec{x_s})}{K} \quad (3)$$

and can be interpreted as the potential at $\vec{x}$ (the observation point) caused by a unit point charge at $\vec{x_s}$ (the source point). We do not use the free space Green's function, but Green's functions which are tailored by boundary conditions additional to Equation (3) for the particular problem. In both the resistance and the capacitance case the result is such that, in Equation (2), all integrals but the third vanish. The properties of the Green's functions will be discussed in the next sections. The derivations can be found in Appendix A and Appendix C. The boundary Γ_1 is discretized into N elements, piecewise constant shape functions are assumed for the unknowns and using the collocation method[4] and our Green's functions, Equation (1) reduces to

$$\alpha u_i = \sum_{j=1}^{N} \left.\frac{\partial u}{\partial n}\right|_{\text{element}_j} \int_{\Gamma_{1,j}} G(\vec{x_i}; \vec{x_j}) d\Gamma_j \,, \quad i = 1, 2, 3, ..., N \quad (4)$$

The integrations can be performed analytically or numerically. For these problems it can be shown that $\alpha = 1$. With the definitions of $\mathbf{U}$ as the vector of N element potentials and $\mathbf{Q}$ as the vector of N unknowns on the elements, the above equation can be written in matrixform as

$$\mathbf{U} = \mathbf{G}\mathbf{Q} \quad (5)$$

The elastance matrix $\mathbf{G}$ now describes the influence between each pair of boundary elements. With the definitions of an incidence matrix $\mathbf{F}$ relating element quantities to conductor quantities, the conductor potential vector $\mathbf{V}$ and the conductor unknowns vector $\mathbf{X}$ we can write

$$\mathbf{U} = \mathbf{F}\mathbf{V} \quad (6)$$

$$\mathbf{X} = \mathbf{F}^T\mathbf{Q} \quad (7)$$

and thus the desired model relation is given by

$$\mathbf{X} = \mathbf{F}^T\mathbf{G}^{-1}\mathbf{F}\mathbf{V} = \mathbf{M}\mathbf{V} \quad (8)$$

3D INTERCONNECTION CAPACITANCE CALCULATIONS

The complex network of interconnections on an integrated circuit can be characterized by a capacitance matrix. This matrix must be known to verify the performance of the circuit before fabrication.[1] For the case of 3-dimensional capacitance calculations, $\mathbf{M} = \mathbf{C}_s$ is the desired capacitance model. The domain is treated as a semi-infinite stratified halfspace, i.e. it consists of layers of constant permittivity and the substrate acts as a groundplane. This is justified for the frequencies of interest ($<$ 1Ghz). The discussion below will necessarily be brief. More details and additional references can be found elsewhere.[5,6]

Green's Function

Since the physical problem is rotationally symmetric, we assume a cylindrical coordinate system with the z-axis through $\vec{x_s}$ and the origin at the groundplane. We then define r and z by $\vec{x} = (z, r)$ and $\vec{x_s} = (z_s, 0)$. In Appendix A it is then derived that the Green's function can be written as

$$G(\vec{x}; \vec{x_s}) = \sum_{n=0}^{\infty} \frac{s_n}{\sqrt{r^2 + (z - z_n)^2}} \quad (9)$$

This Green's function satisfies Equation (1), with the boundary conditions specified in the previous section. Additionally, it satisfies the conditions that the potential and normal component of the electric displacement are continuous across the dielectric interfaces. It can be integrated either analytically[12] or numerically.[13] (Because of the computational complexity of the analytic integration, we use a hybrid integration scheme that first tries a numerical integration and reverts to analytic if it does not converge fast enough.) Thus, $\mathbf{M} = \mathbf{C}_s$ can be calculated by Equation (8).

Model Reduction

However, Equation (8) results in a full matrix which specifies a capacitance between every pair of conductors. For our application, this corresponds to a circuit that contains (too) much irrelevant detail since conductors that are far apart have a negligible (although non-zero) capacitance. Moreover, the computational complexity of the matrix inversion process, $O(N^3)$, would restrict the applicability of the method to situations without practical significance.

What we need is a so-called *reduced* capacitance model where only the important couplings have non-zero values and the unimportant couplings are vanishing. Note that we cannot accomplish this by zeroing small entries in $\mathbf{G}$, since the matrix inversion would produce fill-ins: the inverse of a sparse matrix is, in general, not sparse. Moreover, the result would correspond to a non-physical situation because it would not be positive-definite. On the other hand, merely ignoring small entries in $\mathbf{G}^{-1}$ would not deliver an optimal reduced model nor would it eliminate the computation time bottleneck.

Instead, we will use a Schur-type algorithm to produce an approximate positive definite sparse inverse $\mathbf{G}_{SI}^{-1}$ for a positive definite matrix $\mathbf{G}$ that is specified on a double band S (see Appendix B for details). $\mathbf{G}_{SI}^{-1}$ has zeros on the complement of S and is the exact inverse of the so-called maximum entropy extension of a matrix $\mathbf{G}'$ that is close to $\mathbf{G}$. It has been shown[8] that, under certain conditions, $\mathbf{G}_{SI}^{-1}$ is an optimal reduced model.

Thus, we compute a sparse approximation $\mathbf{G}_{SI}^{-1}$ of $\mathbf{G}^{-1}$, thereby in effect ignoring small capacitances between conductors that physically are 'far' from each other. The distance w, above which capacitances are ignored, is a parameter of the method. This allows to trade detail of the model against computation time.

The algorithm requires $O(Nb^2)$ operations, where N is the number of boundary elements and b is the average number of non-zero entries on a row of $\mathbf{G}_{SI}^{-1}$. This latter quantity is determined by the average number of nearby elements, which does not depend on the problem size but only on the window size w and the mesh granularity. Consequently, the running time is in practice proportional to the size of the problem.

3D SUBSTRATE RESISTANCE CALCULATIONS

The substrate of a VLSI chip may be seen as a multi-terminal distributed resistance network between the contacts on the boundary of the substrate. These contacts may be explicitly designed substrate contacts and e.g. substrate terminals of (active) devices such as MOSFETs. $\mathbf{M} = \mathbf{Y}_{IAM}$ is the desired indefinite admittance matrix of this network. It is important to know this matrix in order to prevent or suppress parasitic coupling via the substrate, which may lead to incorrect behaviour of the designed chip.[2]

Green's Function

We specify the Green's function by demanding homogeneous Neumann boundary conditions on Γ_1 *and* Γ_2 for the fundamental solution. The homogeneous Neumann conditions and the divergence theorem require that the volume integral of the right-hand-side of Equation (3) equals 0. Therefore this equation has to be modified to

$$\nabla^2 G(\vec{x};\vec{x_s}) = -\frac{\delta(\vec{x}-\vec{x_s})}{K} + \frac{1}{KV_\Omega} \tag{10}$$

The last term can be seen as a sink, distributed over the volume V_Ω, with a strength equal to the source at $\vec{x_s}$.

There exist several methods to derive the desired Green's function:[7] full eigenfunction expansion, method of images and the operator technique (also called partial eigenfunction expansion). The former 2 methods both yield an expression for G with a triple infinite sum. The convergence, especially of the first method, is slow. The latter method, however, yields a double infinite sum, which in many cases converges fairly rapidly. Therefore we have chosen to use this method. The derivation of the (modified) Green's function for the layered cuboid by the operator technique and the result (Equations (31) and (32)) are given in Appendix C. We will describe the method for a general multilayer domain and present the results for the important case of 2 layers. This situation occurs in the case of a substrate with an epi-layer, which is very common in mixed analogue-digital IC's.

For a homogeneous medium the result becomes equal to previously obtained results.[9] This form can further be reduced to the 2-dimension Green's function for a homogeneous domain.[10]

Calculation

The sink term in Equation (10) causes a new constant (unknown) term Ψ to appear in Equation (4):

$$\alpha u_i = \sum_{j=1}^{N} \left.\frac{\partial u}{\partial n}\right|_{\text{element}_j} \int_{\Gamma_{1,j}} G(\vec{x_i};\vec{x_j})\, d\Gamma_j + \Psi, \qquad i = 1,2,3,...,N \tag{11}$$

This term is the average potential over the domain. The normal derivative of the potential is related to the current density through the contacts by the local form of Ohm's law. To complete the set of equations, we use the Kirchhoff current law, which states that the sum of all terminal currents equals 0:

$$\sum_{j=1}^{N} A_{\Gamma_j} K \left.\frac{\partial u}{\partial n}\right|_{\text{element}_j} = 0 \tag{12}$$

where A_{Γ_j} is the area of element j. Thus the indefinite admittance matrix of the substrate is given by

$$\mathbf{Y}_{IAM} = \mathbf{F}^T \mathbf{G}_+^{-1} \mathbf{F} \tag{13}$$

Here $\mathbf{G}_+$ results from the matrix $\mathbf{G}$ augmented such that Ψ is the $(N+1)^{\text{th}}$ unknown and the Kirchhoff current law is the $(N+1)^{\text{th}}$ equation and multiplying by a diagonal matrix with the area of the elements as entries. The incidence matrices are modified appropriately.

Due to the form of the series expression for the Green's function the integrals in Equation (11) can be evaluated analytically. Thus also a Galerkin method[4] can be easily implemented and in fact is more efficient than a collocation method. Since matrix $\mathbf{G}$ is symmetric for the Galerkin method only half of the entries has to be computed. This gain is often larger than the evaluation of the additional integrals.

IMPLEMENTATION

The method as described above is implemented in an IC verification program called Space.[3] From a layout description of a chip, Space produces a circuit netlist that contains the interconnect capacitances as well as the active devices and interconnect resistances.

Space incorporates all steps of the method in a single program that performs one single pass over the input data. It reads a layout database and a file containing the relevant technological data, and defines a window that is swept over the layout. Within the window, the mesh is created, the collocation integral is computed for all pairs of boundary elements within the window, the resulting (partially specified) elastance matrix is inverted on the fly, and the approximate inverse is multiplied by the the incidence matrix. The result is merged with the network of active devices and interconnect resistances, and written to a netlist database. This netlist is ready for simulation, e.g. with Spice.[11]

RESULTS

Capacitance calculations

To illustrate the efficiency of the program, consider a layout consisting of two crossing busses of 5 wires each, see Figure 2. The lower conductors are numbered 1-5 and the upper conductors are numbered 6-10. The thickness and width of the conductors, as well as the horizontal and vertical separations are all 1μm. The medium consists of a single semi-infinite dielectric layer with a relative permittivity of 3.9 (SiO_2). The boundary element mesh that is created by Space consists of 460 elements of $1\mu\text{m} \times 1\mu\text{m}$.

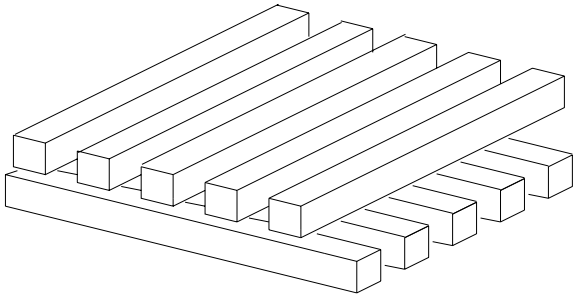

Figure 2: *Crossing-bus example layout.*

Some results of extracting this layout when the window size w is varied, are shown in Table 1. For $w = 11\mu$m, they correspond to an exact inversion of the elastance matrix and this results in a completely specified (i.e. full) capacitance matrix $\mathbf{C}_s$. Note that when a capacitance C_{ij} vanishes, the corresponding ground capacitance $C_{i\,\text{gnd}}$ increases so that the total capacitance of a conductor changes very little. This will ensure accurate delay simulation, at the cost of reduced crosstalk detail. The computation times and memory usage for the above calculations are shown in Table 2. Small values of w thus give acceptable capacitance models, however, with much reduced memory use and CPU times.

Further results, including comparison to results obtained with other programs, are given elsewhere.[5]

Table 1: *Some typical entries from the calculated capacitance matrix as a function of the window size.*

w	capacitances (10^{-18}F)					
(μm)	$C_{1\,\text{gnd}}$	C_{12}	C_{13}	C_{14}	C_{15}	C_{16}
11	453.1	586.6	44.3	17.9	12.3	144.6
5	462.5	585.0	43.3	17.2	11.9	143.9
4	476.0	584.0	43.0	21.3		143.4
3	499.0	582.6	5.0			142.9
2	554.2	599.3				141.4
1	645.4	490.8				139.9

Table 2: *Computation time and Memory usage as a function of the window size, on an HP 9000/720.*

w	time	mem
(μm)	(sec)	(Mbyte)
11	144.5	14.74
5	83.2	4.14
4	47.8	2.10
3	26.8	0.78
2	12.5	0.32
1	3.6	0.14

Resistance Calculations

The accuracy of the method in 2D situations has been established elsewhere.[10] Here we will focus on 3D results. The structure in Figure 3 is calculated without and with the bottom contact. The resulting admittance matrices are shown as $\mathbf{Y}_3$ and $\mathbf{Y}_4$, respectively. Matrix $\mathbf{Y}_3$ can be obtained from $\mathbf{Y}_4$ by Gaussian elimination. We verified that this relation holds for the numerical results, with a maximum error of 0.3%. From the matrices one can see that a substrate contact at the backside of a chip decreases the coupling between points at the surface. In effect, it acts as a sink for the disturbances injected into the substrate.

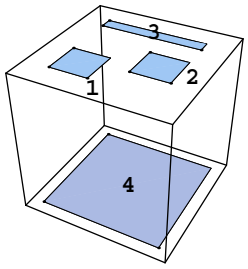

$$\mathbf{Y}_3 = \begin{pmatrix} 4.88081 & -2.4078 & -2.47302 \\ -2.40166 & 5.57079 & -3.16914 \\ -2.47916 & -3.163 & 5.64215 \end{pmatrix}$$

$$\mathbf{Y}_4 = \begin{pmatrix} 5.82148 & -1.51848 & -1.37216 & -2.93084 \\ -1.51529 & 6.4316 & -2.11119 & -2.80512 \\ -1.37397 & -2.0973 & 6.98414 & -3.51287 \\ -2.93223 & -2.81582 & -3.50079 & 9.24884 \end{pmatrix}$$

Figure 3: *3D structure with calculated admittance matrices.*

Figures 4 and 5 show a structure which is typical for actual design problems. The structure represents a 15 Ωcm epi-layer on a good conducting substrate ($\rho = 0.05$ Ωcm). R_{lead} and L_{lead} are realistic estimates of the resistance and inductance of the interconnection and wiring needed to connect the contacts with external IC pins. The outer top contacts (1 and 4) are substrate contacts both 40μm wide and 190μm long. Contact 3 ($50\mu\text{m} \times 180\mu\text{m}$) represents the output (drain implant) of a digital oscillator and contact 2 ($10\mu\text{m} \times 100\mu\text{m}$) a sensitive node in an analog circuit.

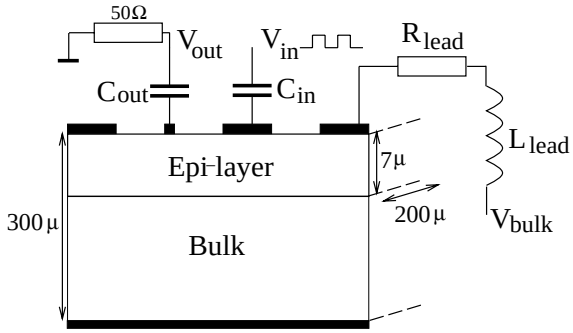

Simulation data:

$V_{\text{in}} = 5$V	$f_{\text{Vin}} = 1$GHz	$C_{\text{in}} = 0.2$pF
$C_{\text{out}} = 0.015$pF	$R_{\text{lead}} = 2\Omega$	$L_{\text{lead}} = 10$nH
$\rho_{\text{epi}} = 15$ Ωcm	$\rho_{\text{bulk}} = 0.05$ Ωcm	$V_{\text{bulk}} = -5$V

Figure 4: *Cross section with of example structure with external components for substrate resistance calculations.*

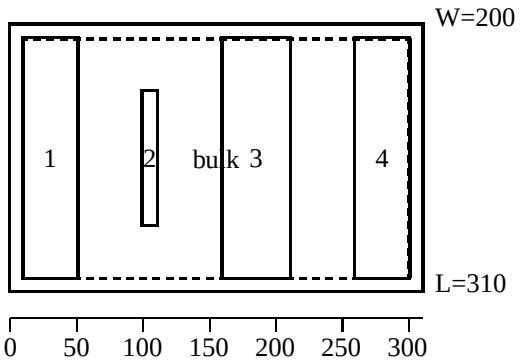

Figure 5: *Top view of example structure for substrate resistance calculations.*

Figure 6 shows results obtained by simulation of the substrate admittance matrix calculated with the method described above together with the external components with SPICE.[11] The simulations are repeated with one or more of the substrate contacts in use. It is clearly seen that the addition of substrate contacts decreases the parasitic coupling. In an IC design it is often a very important question how many substrate contacts are necessary. Too few leads to erroneous circuit behaviour, too many leads to higher costs. With simulations like the above a reliable decision can be made.

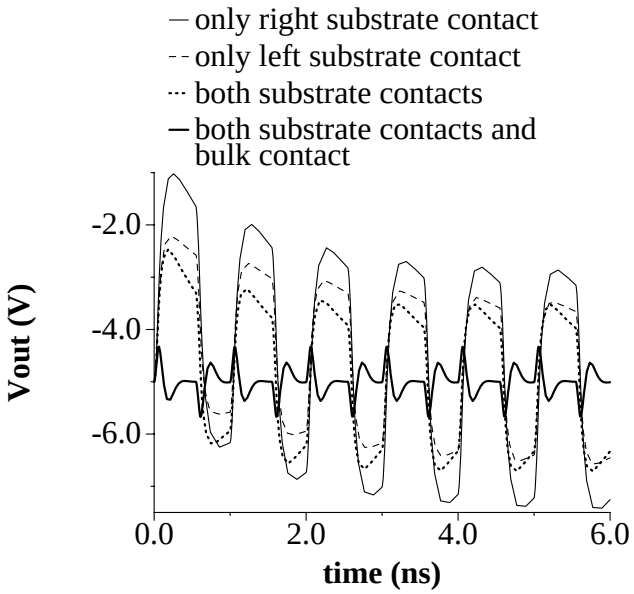

Figure 6: *Results from SPICE of structure from Figure 4.*

CONCLUSIONS

This paper describes Boundary Element Methods for the calculation of interconnection capacitances and substrate resistances for the verification of VLSI designs. The methods use Green's functions tailored to the specific problem, such that a simple integral formulation remains. This formulation is transformed into the desired capacitance and admittance matrices. The approximative inversion of the elastance matrix can be done with linear time complexity with the Schur algorithm. We showed the applicability of the methods by several examples.

Acknowledgement

This research was funded by the Dutch Foundation for Fundamental Research on Matter (FOM) and the Dutch Technology Foundation (STW).

REFERENCES

[1] Bakoglu, H.B. *Circuits, Interconnection and Packaging for VLSI*, Addison-Wesley, Reading, 1990.

[2] Kup, B.M.J. et.al. 'A Bit-stream Digital-to-Analog Converter with 18-b Resolution' *IEEE Journal of Solid-State Circuits*, Vol. 26, No.12, pp. 1757-63, 1991.

[3] Meijs, N.P. van der and Genderen, A.J. van. *Space User's Manual*, Report ET-NT 92.21, Delft University of Technology, Delft, 1992.

[4] Brebbia, C.A. *The Boundary Element Method for Engineers*, Pentech Press, London, 1978.

[5] Meijs, N.P. van der. *Accurate and Efficient Layout Extraction*, PhD thesis, Delft University of Technology, Delft, 1992.

[6] Genderen, A.J. van. *Reduced Models for the Behaviour of VLSI Circuits*, PhD thesis, Delft University of Technology, Delft, 1991.

[7] Zauderer, E. *Partial Differential Equations of Applied Mathematics*, John Wiley & Sons, New York, 1989.

[8] Nelis, H. *Sparse Approximations of Inverse Matrices*, PhD thesis, Delft university of Technology, Delft, 1989.

[9] Smedes, T., Meijs, N.P. van der, Genderen, A.J.van, 'Boundary Element Methods for Capacitance and Substrate Resistance Calculations in a VLSI Layout Verification Package', *Software Applications in Electrical Engineering, Ed.: P.P. Silvester*, pp. 337-344, 1993.

[10] Smedes, T., 'Substrate Resistance Extraction for Physics-based Layout Verification', *Proceedings of the IEEE/ProRISC Workshop on Circuits Systems and Signal Processing*, Houthalen, Belgium, pp. 101-106, 1993.

[11] Quarles, T. et. al. *SPICE 3B1 User's Guide*, University of California, Berkeley, 1991.

[12] Wilton, D.R. et al. 'Potential Integrals for Uniform and Linear Source Distributions on Polygonal and Polyhedral Domains', *IEEE Trans. on Antennas and Propagation*, Vol. AP-32, No 3, pp. 276-281, March 1984.

[13] Stroud, A.H. *Approximate Calculation of Multiple Integrals*, Prentice Hall, Englewood Cliffs, 1971.

[14] Abramowitz, M. and Stegun, I.A. *Handbook of Mathematical Functions*, Dover, New York, 1970.

Appendix A Green's Function for the Capacitance Problem

For the problem of computing the interconnect capacitances, the lateral dimensions of an integrated circuit are very large when compared to the relevant vertical dimensions. Therefore, we may neglect the effect of the boundaries of the chip and treat the problem as being rotationally symmetric. Thus, we assume the physical situation to be rotationally symmetric around $\vec{x_s}$. Thus we can write Equation (1) in cylindrical coordinates with the z-axis through $\vec{x_s}$ and the origin at the groundplane. Then, we have $\vec{x} = (r, z)$ and $\vec{x_s} = (0, z_s)$. By separation of variables we obtain $G = Z(z; z_s)R(r)$, where

Z satisfies the hyperbolic (second order) ODE and R satisfies the Bessel equation of order zero. When this system is solved, the solution containing the Bessel function of the second kind is rejected because of the boundary conditions. The Green's function can now be written as a linear combination of the independent solutions as:

$$G = \int_0^\infty \left(A(m)e^{m(z-z_s)} + B(m)e^{m(z_s-z)} \right) J_0(mr)dm \tag{14}$$

The A and B can be determined by applying the boundary and continuity conditions, as we will illustrate below. The result will be a series solution. However, we have found that a more efficient series solution will result when we write G as the sum of the Green's function for a semi-infinite halfspace with a groundplane and dielectric layer 1 (with permittivity K_1) only and a term for the dielectric interfaces as follows:

$$G = \frac{1}{4\pi K_1}\left(\frac{1}{\sqrt{r^2+(z-z_s)^2}} - \frac{1}{\sqrt{r^2+(z+z_s)^2}} \right) + \int_0^\infty \left(A(m)e^{m(z-z_s)} + B(m)e^{m(z_s-z)} \right) J_0(mr)dm \tag{15}$$

The solution of this equation proceeds as follows. Let there be N_d dielectric layers. We assume that $N_d \geq 2$, if $N_d = 1$ we would have $A(m) = B(m) = 0$. The Green's function will then consist of N_d^2 branches G_{ij}, corresponding to $\vec{x_s}$ in dielectric layer i and $\vec{x}$ in layer j. (Of course, because of symmetry, only $N_d(N_d+1)/2$ branches will be distinct.) Now, let $\vec{x_s}$ be situated in layer i. Imposing the boundary and continuity conditions then gives $2N_d$ equations in A_{ij} and B_{ij}, which can be solved to yield A_{ij} and B_{ij} for $1 \leq j \leq N_d$. This procedure can be repeated for all i with $1 \leq i \leq N_d$, to determine all A_{ij} and B_{ij}.

The A_{ij} and B_{ij} are rational expressions of the form

$$\frac{\sum_x a_x e^{p_x m}}{1+\sum_y b_y e^{q_y m}} \tag{16}$$

where a_x, and b_y depend on the medium and p_x and q_y depend on the medium and z_s. These can be converted into a power series, and expanding this series and also using the identity[14]

$$\int_0^\infty e^{-am} J_0(bm)dm = \frac{1}{\sqrt{a^2+b^2}}, \qquad a > 0, \tag{17}$$

we can evaluate the integral in Equation (15)

$$\int_0^\infty (.) J_0(mr)dm = \sum_{n=0}^{\infty} \sum_t \frac{s_{n\,t}}{\sqrt{r^2+(z-z_{n\,t})^2}} \tag{18}$$

in which the summation over t is finite. However, in the case of more than 2 dielectric layers, the number of terms in this summation increases rapidly with n. To reduce the associated computation time, we are currently investigating an approximation scheme in which we evaluate a small number of terms of the summation over n exactly, and use a table-lookup/interpolation scheme to approximate the remainder. We have indications that this approach works well, as can be expected because the remainder is a very smooth function of r, z and z_s.

For a physical interpretation Equation (18) can be inserted into Equation (15). After rearranging of terms the resulting Green's function is algebraically equivalent to

$$G(\vec{x};\vec{x_s}) = \sum_{n=0}^{\infty} \frac{s_n}{\sqrt{r^2+(z-z_n)^2}} \tag{19}$$

The s_n and z_n can be interpreted as the image coefficients and positions, respectively.[7] In particular, $s_0 = 1/(4\pi K)$ and $z_0 = z_s$, so that the 0'th term is the free-space solution u^*. Also, $s_1 = -1/(4\pi K)$ and $z_1 = -z_s$, so that the 1'st term is the groundplane mirror image of z_s.

Appendix B The Hierarchical Schur Algorithm

The Hierarchical Schur Algorithm to extract 3D capacitances of interconnects in VLSI layouts is described as follows:

1. Divide the layout into vertical strips of width w (see Figure 7). All direct influences between elements that are within a distance w will be computed.

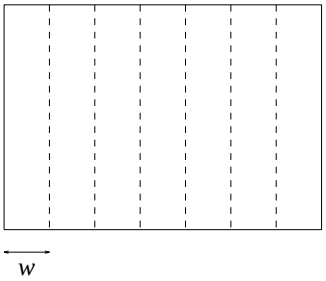

Figure 7: *A layout divided into vertical strips of width* w.

2. For each *single* strip, except for the first strip and the last strip, and for each *pair of adjacent* strips: (a) compute a partially specified elastance matrix **G**, where only entries G_{ij} of **G** are computed for which element i and element j are — measured along the long side of the strips — within a distance w of each other, (b) compute the inverse of the so-called maximum entropy extension of **G**, using the generalized Schur algorithm as described below,[8] and (c) derive a short-circuit capacitance matrix from this matrix (as in Equation (8)).

3. For each *pair* of strips, the result of step 2 is added to the short-circuit capacitance matrix for the total circuit. For each *single* strip, the result of step 2 is subtracted from the short-circuit capacitance matrix for the total circuit.

Note that, in the above, the complete sparse approximation $\mathbf{G}_{SI}^{-1}$ of **G** never exists as a whole, but that the short-circuit capacitance matrix **M** is incrementally computed from the results for the (pairs of) strips.

The generalized Schur algorithm

Input: a positive definite symmetrical matrix $\mathbf{G}$ of size $N \times N$ that is specified on a staircase band S.

Output: the maximum entropy inverse $\mathbf{G}_{ME}^{-1}$ of $\mathbf{G}$ ($\mathbf{G}_{ME}$ coincides with $\mathbf{G}$ on S and $\mathbf{G}_{ME}^{-1}$ has zeros on the complement of S).

Method:

1. Let $\mathbf{D}$ be the diagonal matrix $[G_{11}\, G_{22} \ldots G_{NN}]$. Let $\mathbf{G}_n$ be the normalization $\mathbf{D}^{-1/2}\ \mathbf{G}\ \mathbf{D}^{-1/2}$ of $\mathbf{G}$, such that $[G_{nii}] = 1$, $i = 1 \ldots N$.

2. Let $\mathbf{V}$ be a strictly upper triangular matrix, such that $\mathbf{G}_n = \mathbf{V} + \mathbf{I} + \mathbf{V}^*$, and let $\mathbf{U} = \mathbf{V} + \mathbf{I}$.

3. Let $\boldsymbol{\Theta}$ be a $2N \times 2N$ identity matrix.

4. **For** $(i,j) \in \{S \mid V_{ij} \neq 0\}$ in diagonal-major order **do**

$$\begin{array}{rcl} [\mathbf{U}\ \mathbf{V}] & = & [\mathbf{U}\ \mathbf{V}]\,\theta(i,j) \\ \Theta & = & \Theta\theta(i,j). \end{array} \tag{20}$$

   Here, $\theta(i,j)$ is an elementary hyperbolic rotation matrix as defined below, such that V_{ij} is eliminated. The diagonal-major order of entries to be eliminated is as follows: first the first non-zero entry of the first diagonal, then the second non-zero entry, etc. If the first diagonal of $\mathbf{V}$ has been eliminated, proceed with the second diagonal, and so on.

5. Compute the triangular factors $\mathbf{L}^{-*}$ and $\mathbf{M}^{-1}$ of the maximum entropy inverse of $\mathbf{G}_n$:

$$[\mathbf{L}^{-*}\ \mathbf{M}^{-1}] \ = \ [\mathbf{I}\ \mathbf{I}]\ \Theta. \tag{21}$$

6. Evaluate ${\mathbf{G}_n^{-1}}_{ME}$ and denormalize, resulting in $\mathbf{G}_{ME}^{-1}$:

$$\begin{array}{rcl} \mathbf{G}_{ME}^{-1} & = & \mathbf{D}^{-1/2}\mathbf{L}^{-*}\ \mathbf{L}^{-1}\ \mathbf{D}^{-1/2} \\ & = & \mathbf{D}^{-1/2}\,\mathbf{M}^{-1}\,\mathbf{M}^{-*}\,\mathbf{D}^{-1/2}. \end{array} \tag{22}$$

In the above algorithm, $\theta(i,j)$ is a $2N \times 2N$ identity matrix, except for the following entries:

$$\begin{array}{rcl} \theta(i,j)_{i,i} & = & (1-|\rho|^2)^{-1/2} \\ \theta(i,j)_{i,j+N} & = & \rho(1-|\rho|^2)^{-1/2} \\ \theta(i,j)_{j+N,i} & = & \rho^*(1-|\rho|^2)^{-1/2} \\ \theta(i,j)_{j+N,j+N} & = & (1-|\rho|^2)^{-1/2}, \end{array} \tag{23}$$

where the reflection coefficient ρ ($|\rho| < 1$) is given by $\rho = -V_{ij}/U_{ii}$. An efficient implementation of this algorithm has been described elsewhere.[6]

Appendix C Green's Function for the Resistance Problem

In this appendix we present the derivation of the modified Green's function for the layered cuboid ($0 \le x \le L, 0 \le y \le W, 0 \le z \le H$). The domain is illustrated in Figure 8. Here we treat the case with two layers, but the method can easily be extended to any number of layers.

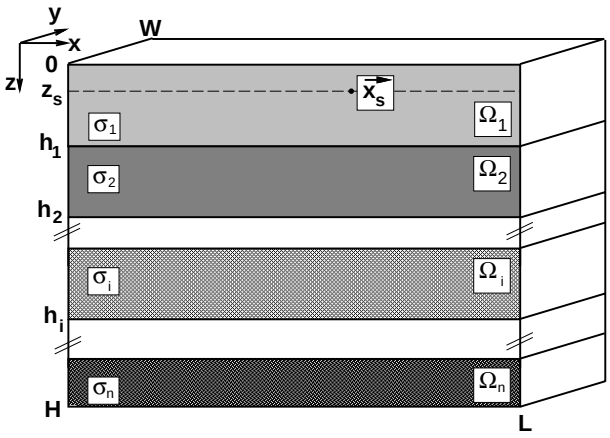

Figure 8: *Layered domain for Green's function.*

The Green's function has to satisfy Equation (10) with homogeneous Neumann conditions on all boundaries. Furthermore we need additional properties to describe the behaviour of the Green's function at the interfaces between 2 layers with different conductivity. We impose continuity of the Green's function and continuity of the normal flux ($\sigma \partial G/\partial z$) at each interface. An efficient form of the Green's function is found by the operator technique.[7] This method is summarized as follows:

1. Rewrite Equation (10) as

$$\frac{\partial^2 G(\vec{x};\vec{x_s})}{\partial z^2} - \mathsf{L}G(\vec{x};\vec{x_s}) = -\frac{\delta(\vec{x}-\vec{x_s})}{K} + \frac{1}{KV_\Omega} \tag{24}$$

   with the operator $\mathsf{L} = -\left(\partial^2/\partial x^2\right) - \left(\partial^2/\partial y^2\right)$

2. Find a complete orthonormal set of eigenfunctions $K_{mn}(x,y)$ for operator L

3. Expand $G(\vec{x};\vec{x_s})$ in these eigenfunctions

$$G(\vec{x};\vec{x_s}) = \sum_{m,n=0}^{\infty} N_{mn}(z;\vec{x_s}) K_{mn}(x,y) \tag{25}$$

4. Substitute this in Equation (24) and use the eigenfunction property.

5. Multiply the result by $K_{mn}(x,y)$ and integrate over the domain of L

6. Use Green's identity to obtain an ordinary differential equation for N_{mn}

$$\begin{aligned} &N''_{mn}(z;\vec{x_s}) - \lambda_{mn} N_{mn}(z;\vec{x_s}) = \\ &-\frac{K_{mn}(x_s,y_s)\delta(z-z_s)}{K} + \int_0^L \int_0^W \frac{K_{mn}(x,y)}{KV_\Omega} dx\,dy \end{aligned} \tag{26}$$

7. Solve this equation for $N_{mn}(z;\vec{x_s})$

The required set of eigenfunctions is given by

$$K_{mn}(x,y) = \sqrt{\frac{\gamma_{mn}}{LW}} \cos\left(\frac{m\pi x}{L}\right) \cos\left(\frac{n\pi y}{W}\right) \quad (27)$$

with

$$\gamma_{00} = 1, \gamma_{m0} = \gamma_{0n} = 2, \gamma_{mn} = 4 \quad (28)$$

and eigenvalues

$$\lambda_{mn} = \left(\frac{m\pi}{L}\right)^2 + \left(\frac{n\pi}{W}\right)^2 \qquad m,n = 0,1,2,3,... \quad (29)$$

The last step of the above procedure needs some concern. For $mn \neq 00$ the last term of Equation (26) disappears. We can then solve 2 homogeneous PDE's the layer containing the source point ($z < z_s$ and $z > z_s$) and 1 homogeneous PDE for each other layer. the general solution of each of these equations is

$$N_{mn}(z;\vec{x_s}) = A\cosh\left(\sqrt{\lambda_{mn}}z\right) + B\sinh\left(\sqrt{\lambda_{mn}}z\right) \quad (30)$$

The $(2n+2)$ unknowns can be found from the boundary conditions, the continuity conditions at the interfaces and the continuity and jump condition at $z = z_s$.

For $mn = 00$ the last term of Equation (26) is easily evaluated. The solution in this case is then found by simple integrations in the layer containing the source point (for $z < z_s$ and $z > z_s$) and the other layers. The solutions are coupled in the same manner as above. However, the jump condition is automatically satisfied, which leads to an integration constant in N_{00}.

For a Green's function describing all possible positions of the source point this procedure has to be repeated for $\vec{x_s}$ in all layers. However for several applications it is not necessary to specify the complete function. In particular in our application, $\vec{x}$ and $\vec{x_s}$ are always in the top most or bottom most layer, since contacts cannot be defined inside the IC. Therefore explicit formulation of the 'inner branches' can be avoided.

Finally, we give the results for the modified Green's function of a 2 layer structure with the source point in the first layer. The coefficients in Equation (25) are then given by

$$\frac{N_{00}^{(1)}}{K_{00}(x_s,y_s)} = \begin{cases} \frac{z^2}{2\sigma_1 H} - \frac{z_s}{\sigma_1} + K, & \text{if } 0 < z < z_s \\ \frac{z^2}{2\sigma_1 H} - \frac{z}{\sigma_1} + K, & \text{if } z_s < z < h \\ \frac{z^2-h^2}{2\sigma_2 H} - \frac{z-h}{\sigma_2} + \frac{h^2-2hH}{2\sigma_1 H} + K, & \text{if } h < z < H \end{cases} \quad (31)$$

and

$$\frac{N_{mn}^{(1)}}{K_{mn}(x_s,y_s)} = \begin{cases} \frac{(C(H-z_s)+\Delta C(H-2h+z_s))C(z)}{S(H)-\Delta S(H-2h)}, & \text{if } 0 < z < z_s \\ \frac{(C(H-z)+\Delta C(H-2h+z))C(z_s)}{S(H)-\Delta S(H-2h)}, & \text{if } z_s < z < h \\ \frac{2\sigma_1 C(z_s)C(H-z)}{(\sigma_1+\sigma_2)S(H)-(\sigma_1-\sigma_2)S(H-2h)}, & \text{if } h < z < H \end{cases} \quad (32)$$

where we have defined the auxiliary notations

$$C(x) = \cosh\left(\sqrt{\lambda_{mn}}x\right), \quad S(x) = \sinh\left(\sqrt{\lambda_{mn}}x\right) \quad (33)$$

and

$$\Delta = \frac{\sigma_1 - \sigma_2}{\sigma_1 + \sigma_2} \quad (34)$$